

# Weighted Circular Folding Cooperative Power Spectral Density Split Cancellation Algorithm

Lucas S. Costa, Dayan A. Guimarães, Edilson P. Frigieri, and Rausley A. A. de Souza, *Senior Member, IEEE*,

**Abstract**—Low computation complexity and robustness against dynamical noise are attributes of the cooperative power spectral density split cancellation (CPSC) algorithm, developed for centralized data-fusion cooperative spectrum sensing. Recently, an improved version of the CPSC was proposed, named circular folding CPSC (CFCPSC), which outperforms the CPSC while maintaining low complexity and robustness against dynamical noise. This correspondence proposes the weighted CFCPSC (WCFCPSC), which improves the performance of the CFCPSC, retaining the attributes of its predecessors. Expressions are derived for the probability of false alarm, and for the probability density and the cumulative distribution functions of the main random variables that form the WCFCPSC test statistics. Simulations results are given to support the theoretical findings and to demonstrate the superior performance of the WCFCPSC.

**Index Terms**—CFCPSC, cognitive radio, cooperative spectrum sensing, CPSC, dynamic spectrum access, WCFCPSC.

## I. INTRODUCTION

THE problem of radio-frequency (RF) spectrum shortage is a consequence of the unprecedented growth in wireless communications services and the adoption of the fixed spectrum allocation policy in which the incumbents, often called primary users (PUs), are granted exclusive right to use a given band. This growth will become even more pronounced due to the deployment of the fifth-generation (5G) of wireless communication systems and the proliferation of the Internet of things (IoT), as both will interconnect a massive number of transceivers.

Nonetheless, researches have revealed that the RF spectrum is underutilized in certain bands and geographic locations [1]. Hence, a new dynamic spectrum access (DSA) policy has been considered as a solution to the RF spectrum shortage problem. In this new policy, secondary users (SUs) can share the RF spectrum with the PUs, for instance by means of opportunistic access to vacant bands. This is accomplished by means (or with the help) of spectrum sensing [2], a technique that renders the SUs the capability of searching for idle bands.

Challenges, opportunities and applications of the spectrum sensing in the context of vehicular networks is given for instance in [3, Chap. 8].

This work was supported in part by CNPq under Grant 308365/2017-8 and in part by RNP, with resources from MCTIC, Grant 01250.075413/2018-04, under the Radiocommunication Reference Center (*Centro de Referência em Radiocomunicações* - CRR) project of the National Institute of Telecommunications (*Instituto Nacional de Telecomunicações* - Inatel), Brazil.

L. S. Costa, D. A. Guimarães and R. A. A. de Souza are with Inatel, Av. João de Camargo, 510, Santa Rita do Sapucaí, 37540-000, MG, Brazil. E. P. Frigieri is with ASML, De Run 6501, Veldhoven 5504DR, The Netherlands (e-mail: lucass@inatel.br; dayan@inatel.br; rausley@inatel.br; edilson.frigieri@asml.com).

Cooperative spectrum sensing (CSS), which makes use of multiple SUs that collaborate in the PU signal detection process, offers better detection performances than its non-cooperative counterpart, while mitigating multipath fading, shadowing, and the hidden terminal problem [2].

In centralized CSS, which is the focus of this correspondence, the SUs in cooperation collect samples of the received signal and forward them, or some quantity derived from them, to a fusion center (FC) via a report control channel. The FC then combines the received information and makes the decision upon the occupation state of the sensed band.

Among the CSS schemes, the cooperative power spectral density split cancellation (CPSC) [4] has become attractive due to its low computation complexity and robustness against dynamical noise, a situation in which the noise powers at the SUs receivers may be different from each other and time-varying. An improved version of the CPSC called circular folding CPSC (CFCPSC) was recently proposed [5], yielding higher statistical power than its predecessor, while keeping low complexity and robustness against dynamical noise.

The CPSC, the CFCPSC and other related algorithms have been addressed by other research initiatives [6]–[9]. The cumulative distribution functions (CDFs) of the main random variables that form the CPSC test statistics were derived in [6], along with an accurate expression for the probability of false alarm. In [7], the CFCPSC was modified to operate with SUs having multiple antennas. A soft-decision CFCPSC-based algorithm was proposed in [8], and evaluated under quantization errors in the report control channel. In [9], two CFCPSC-based hard decision algorithms were proposed to reduce the report channel data traffic.

This correspondence proposes a modified CFCPSC algorithm in which the test statistics are weighted to form the final statistics. The new algorithm is named weighted CFCPSC (WCFCPSC). Near-optimal and suboptimal weights are proposed and compared. Results show that the WCFCPSC yields a remarkable performance gain over the pure CFCPSC algorithm, maintaining the other attributes of the basis algorithm. An expression for the probability of false alarm is also derived and verified by computer simulations.

## II. SYSTEM MODEL AND THE CFCPSC ALGORITHM

The CSS is made by  $U$  SUs, each one collecting  $N$  samples of the signal received during a sensing interval. These samples are represented by  $x_u(n)$ , for  $n = 1, 2, \dots, N$  and  $u = 1, 2, \dots, U$ . The decision is usually modeled as a binary hypothesis test in which the presence and the absence of

the PU signal are respectively represented by the hypotheses  $\mathcal{H}_1$  and  $\mathcal{H}_0$ . Mathematically,  $x_u(n) = \eta_u(n)$  under  $\mathcal{H}_0$  and  $x_u(n) = s(n) + \eta_u(n)$  under  $\mathcal{H}_1$ , where  $\eta_u(n)$  represents the  $n$ -th sample of a zero-mean additive white Gaussian noise (AWGN) with variance  $\sigma^2$ , and  $s(n)$  denotes the PU signal.

The steps of the CFCPSC algorithm [5] are, in summary:

- 1) Estimate the power spectral density (PSD) of  $x_u(n)$  via the discrete Fourier transform (DFT) according to  $F'_u(n) = \frac{1}{N} |\text{DFT}\{x_u(n)\}|^2$ ;
- 2) Compute the modified circular-even component of  $F'_u(n)$  as  $F_u(n) = (F'_u(1) + F'_u(N/2 + 1))/2$  for  $n = 1$ , and as  $F_u(n) = (F'_u(n) + F'_u(N - n + 2))/2$  for  $n = 2, 3, \dots, N$ ;
- 3) Split  $F_u(n)$  into  $2L$  sub-bands, each having  $V = N/(2L)$  samples, and then compute the quantity  $F_{u,\ell} = \sum_{n=1}^V F_u((\ell - 1)V + n)$  for the  $\ell$ -th sub-band,  $\ell = 1, 2, \dots, L$ ;
- 4) Compute the total signal power received by the  $u$ -th SU via  $F_u^{\text{full}} = \sum_{n=1}^{N/2} F_u(n)$ ;
- 5) Compute the quantity  $r_{u,\ell} = F_{u,\ell}/F_u^{\text{full}}$  for the  $\ell$ -th sub-band monitored by the  $u$ -th SU;
- 6) At the FC, average  $r_{u,\ell}$  over all SUs in the  $\ell$ -th sub-band, yielding the test statistics  $r_\ell^{\text{avg}} = \frac{1}{U} \sum_{u=1}^U r_{u,\ell}$ ;
- 7) Compare  $r_\ell^{\text{avg}}$  with a decision threshold  $\gamma$  and make a decision regarding the  $\ell$ -th sub-band as  $\mathcal{H}_0$  if  $r_\ell^{\text{avg}} < \gamma$ , or  $\mathcal{H}_1$  otherwise;
- 8) Make the decision on the occupation state of the sensed band as  $\mathcal{H}_0$  if all sub-bands were decided as  $\mathcal{H}_0$ ; or as  $\mathcal{H}_1$  if one or more sub-bands were decided as  $\mathcal{H}_1$ .

### III. THE WEIGHTED CFCPSC ALGORITHM

In the WCFCPSC algorithm, the Steps 1, 2, 3, 4, 5 and 8 of the basis CFCPSC algorithm are kept unchanged, whereas the Step 6 is modified such that a weight  $w_\ell$  is applied to the  $\ell$ -th statistic  $r_\ell^{\text{avg}}$ , yielding

$$r_\ell^{\text{avg-w}} = w_\ell r_\ell^{\text{avg}}, \quad (1)$$

from where the factor  $1/U$  used in the computation of  $r_\ell^{\text{avg}}$  can be removed or incorporated into  $w_\ell$ , as it does not influence performance. In the Step 7,  $r_\ell^{\text{avg}}$  is replaced by  $r_\ell^{\text{avg-w}}$ .

#### A. Near-optimal weights

A suitable procedure for determining the optimal weights would be, for example, by maximizing the probability of detection,  $P_d$ , for a fixed probability of false alarm,  $P_{fa}$ , in the optimization variables  $w_\ell$ . However, this is not possible because an expression for  $P_d$  is unknown. Even if such an expression were known, there would be no guarantee that the optimization problem instance could be solved via traditional analytical methods or numerically.

Evidences based on observations of the WCFCPSC performance showed that higher weights must be given to the portions of the received signal plus noise PSD having higher levels. This is an intuitively-satisfying rule, because, in essence, the CPSC-based algorithms detect the PU signal based on the

power concentration difference between the noise-only and the signal plus noise PSDs. Thus, it is claimed that the near-optimal weights are those that follow the shape of the signal plus noise PSD, taking into consideration the circular folding operation in Step 2 of the WCFCPSC algorithm.

Aiming at illustrating the calculation of such near-optimal weights, Fig. 1 shows the PSD of a baseband quaternary phase-shift keying (QPSK) signal, the PSD of the QPSK signal plus noise, and the weights, using hypothetical frequency and PSD values without loss of generality. The weights shown are for  $L = 10$ , with  $w_1$  shifted away from the theoretical QPSK plus noise PSD due to the circular folding operation in Step 2 of the algorithm for  $n = 1$ . Notice that the role of the weights is to favor higher values of  $r_\ell^{\text{avg}}$ , which carry higher signal-to-noise ratios (SNRs), while attenuating the ones corresponding to the tail of the PSD, which are subjected to lower SNRs.

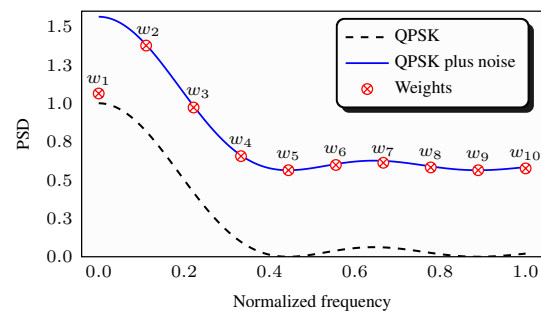


Fig. 1: Illustration of near-optimal weights for the WCFCPSC algorithm.

Since the mathematical proof of the strict optimality or even the near-optimality of the weights is not possible due to the reasons already mentioned, an empirical proof [10] was carried out, from which it can be demonstrated that the PSD-shaped weights can be considered near-optimal if: i) only a few sets of weights can yield better spectrum sensing performances, and ii) when such better performances are attained, they carry small advantages with respect to the one achieved with the claimed near-optimal weights.

To conduct such an empirical proof, 100,000 Monte Carlo simulation trials were executed, each one generating  $L$  independent and uniformly distributed values of  $w_\ell$  in the interval  $[0, 1]$ , yielding the associated spectrum sensing performance in terms of the area under the receiver operating characteristic (ROC) curve, the AUC, obtained from 100,000 spectrum sensing events.

A baseband QPSK PU signal with  $S$  equally-spaced samples per symbol was adopted as the primary user signal. Different values of  $S$  have been tested to simulate different degrees of PSD concentration. A larger  $S$  means a higher PSD concentration.

The number of SUs was set to  $U = 5$ , adopting twelve pairs of  $L$  and  $S$  values:  $S = 4$  with  $L = 10, 20, 40, 80$ ;  $S = 5$  with  $L = 10, 20$ ;  $S = 8$  with  $L = 40, 80$ ;  $S = 10$  with  $L = 10, 20$ ; and  $S = 16$  with  $L = 40, 80$ . Since the number of samples  $N = 2L$  has a large influence on the spectrum sensing performance, the average SNRs across the SUs were set to  $\Gamma = -6.46, -8.93, -11.74, -13.4$  dB, respectively for  $L = 10, 20, 40, 80$ , yielding approximately the same maximum AUC of  $\approx 0.95$  for any  $N$ , which happens in the situation of

maximum PSD concentration, i.e., when the largest value of  $S$  is adopted.

A set having 100,000 AUCs obtained in the above way was generated, for each  $(L, S)$  pair. Each AUC under test was compared with the average of the 50,000 near-optimal AUCs, i.e., those achieved with the PSD-shaped weights, each obtained from 100,000 sensing events. The average has been used to reduce the intrinsic random variations of the AUCs due to the random variables involved in the Monte Carlo simulation of each sensing round, even if the weights are fixed.

Table I shows the percentages (with respect to 100,000 trials) of sensing events in which the AUC with randomized weights surpassed the claimed near-optimal ones. These percentages correspond to the upper values in each cell of the table. The table also shows the AUCs achieved with the near-optimal weights and the maximum AUCs obtained with the random weights, which are respectively the middle and the lower values in each cell of the table. Notice that the percentages are zero or very small. Not coincidentally, the occurrences of nonzero percentages are associated to smaller values of  $L$ , which can be credited to the poor resolution of the weights with regard to represent the true noisy signal PSD. Nonzero values are also influenced by the already-mentioned random fluctuations of the estimated AUCs.

TABLE I: Percentages of events in which the performance with randomized weights surpassed the near-optimal ones. The near-optimal AUCs and the maximum AUCs produced by randomized weights are also given.

$L \backslash S$		4	5	8	10	16
10	%	0.042	0.059		0.225	
	near-optimal	0.862	0.900	-	0.947	-
	maximum	0.867	0.907		0.950	
20	%	0	0		0.008	
	near-optimal	0.824	0.869	-	0.947	-
	maximum	0.814	0.866		0.951	
40	%	0.001		0		0
	near-optimal	0.711	-	0.869	-	0.948
	maximum	0.715		0.856		0.942
80	%	0		0		0
	near-optimal	0.655	-	0.829	-	0.947
	maximum	0.653		0.797		0.909

Based on Table I, one can conclude that the PSD-shaped weights are indeed not optimal, since better performances were found in some trials. Nonetheless, the PSD-shaped weights can be considered near-optimal due to the small number of times that better results were attained, and due to the fact that the maximum AUCs obtained with random weights surpassed the near-optimal ones in a very small amount.

In a statistical sense, it can be stated that the near-optimal PSD-shaped weights are better, on average, than any other randomly chosen set of weights, thus being optimal on average. To support this statement, the following hypothesis test has been formulated and tested:

$$\begin{aligned} H_{\text{null}} &: \mu_{\text{r}} \geq \mu_{\text{o}} \\ H_{\text{alt}} &: \mu_{\text{r}} < \mu_{\text{o}} \end{aligned} \quad (2)$$

where the alternative hypothesis,  $H_{\text{alt}}$ , states that the mean of the AUCs obtained with random weights,  $\mu_{\text{r}}$ , does not surpass the mean of the near-optimal AUCs,  $\mu_{\text{o}}$ . The null hypothesis,  $H_{\text{null}}$ , states the opposite. This test was performed with Minitab, which is a software tool for statistical computing and visualization, applying the one-tailed unequal-variance

two-sample Student's  $t$ -test [11], at the significance level of 0.01, from 100,000 values of the AUCs under test for each of the twelve CSS configurations, and 50,000 values of the corresponding near-optimal AUCs. Table II gives  $p$ -values and absolute  $t$ -values obtained from the test. Since all  $p$ -values are zero, the null hypothesis is rejected, i.e., there is sufficient statistical evidence that  $\mu_{\text{r}} < \mu_{\text{o}}$ . The very high  $t$ -values reinforce this evidence, since they indicate that the differences between the means are much larger than the variability of the samples. Notice also that smaller  $t$ -values correspond to higher percentages in Table I, as expected.

TABLE II:  $p$ -values and  $t$ -values,  $(p, t)$ , associated to the hypothesis test (2).

$L \backslash S$	4	5	8	10	16
10	(0, 631)	(0, 595)	-	(0, 516)	-
20	(0, 861)	(0, 815)	-	(0, 637)	-
40	(0, 1064)	-	(0, 1048)	-	(0, 783)
80	(0, 1259)	-	(0, 1418)	-	(0, 1036)

### B. Heuristic suboptimal weights

In order to determine the near-optimal weights, one must know the received signal plus noise PSD, which in practice is difficult due to the main reasons: i) the modulation and symbol rate adopted by the primary network are usually unknown, possibly changing over time due to the use of adaptive modulation; ii) the noise variance at the SUs receivers is unknown and should be estimated, or the composite received signal plus noise PSD should be estimated. Given the short time-frame of the spectrum sensing, any estimation process would suffer from accuracy degradation and increase the receiver complexity. Notably, these obstacles are in conflict with secondary network premises, since this network should be able to operate autonomously with no PU signal information and, preferably, having low complexity terminals.

Given the above difficulty, alternative near-optimal or sub-optimal weights must be sought. A simple heuristic way of favoring the higher values of  $r_{\ell}^{\text{avg}}$  while attenuating the values corresponding to the PSD tail is to adopt linearly decaying suboptimal weights, that is,

$$w_{\ell} = \frac{L - \ell + 1}{L}. \quad (3)$$

The numerical results given in Section V show that these suboptimal weights yield performances very close to the ones achieved with the near-optimal PSD-shaped weights.

## IV. ANALYTICAL RESULTS

Expressions for the probability density functions (PDFs) and the CDFs of  $r_{\ell}^{\text{avg}}$ , conditioned on  $\mathcal{H}_0$ , were derived in [5], where it is shown that this variable closely follows a Beta distribution with parameters  $\alpha = 2VU$  and  $\beta = (N - 2V)U$ .

Specifically, the conditional CDF of  $r_{\ell}^{\text{avg}}$ , removing the  $\mathcal{H}_0$  conditioning for notational simplicity, is  $F_{r_{\ell}^{\text{avg}}}(x) = \Pr[r_{\ell}^{\text{avg}} < x] = I_x(\alpha, \beta)$ , for  $0 < x < 1$ , where  $I_x(\alpha, \beta)$  is the incomplete regularized Beta function [12, Eq. (8.392)]. The conditional PDF of  $r_{\ell}^{\text{avg}}$  is  $f_{r_{\ell}^{\text{avg}}}(x) = x^{\alpha-1}(1-x)^{\beta-1}/B(\alpha, \beta)$ , where  $B(\alpha, \beta)$  denotes the Beta function [12, p. 908].

Consider the random vector  $\mathbf{r}^{\text{avg}} = [r_1^{\text{avg}}, \dots, r_L^{\text{avg}}]^T$ , where  $[\cdot]^T$  denotes transposition. Assuming uncorrelated variables, the joint PDF and the joint CDF can be written as  $f_{\mathbf{r}^{\text{avg}}}(x_1, \dots, x_L) = \prod_{\ell=1}^L f_{r_\ell^{\text{avg}}}(x_\ell)$  and  $F_{\mathbf{r}^{\text{avg}}}(x_1, \dots, x_L) = \prod_{\ell=1}^L F_{r_\ell^{\text{avg}}}(x_\ell)$ , respectively. Thus, the probability of false alarm is  $P_{\text{fa}} = 1 - F_{\mathbf{r}^{\text{avg}}}(\gamma, \dots, \gamma) \triangleq 1 - F_{\mathbf{r}^{\text{avg}}}(\gamma)$ , with  $x_1, \dots, x_L$  being the decision threshold  $\gamma$ , i.e.  $x_\ell = \gamma$ .

It is worth mentioning that the exact probability of false alarm derived in [5] is given in an  $(L - 1)$ -fold integral of the multivariate generalization of the Beta distribution, which makes the numerical computations of  $P_{\text{fa}}$  extremely cumbersome, if not impossible, specially for high values of  $L$ . This fact is, in itself, a motivation to seek for new expressions or new computational techniques, particularly those that are independent of the value of  $L$ .

In the CPSC and CFCPSC algorithms, the correlation coefficient between any pair  $(r_i^{\text{avg}}, r_k^{\text{avg}})$ ,  $i, k = 1, 2, \dots, L$ ,  $i \neq k$ , is  $\rho_{i,k} = -1/(L - 1)$  [5], [6], which is the same for any pair  $(r_i^{\text{avg-w}}, r_k^{\text{avg-w}})$  for the WCFCPSC, since the deterministic weights do not affect correlation. Although zero correlation does not necessarily imply independence, whereas the converse is true, it is assumed that  $r_i^{\text{avg}}$  and  $r_k^{\text{avg}}$  are independent for  $i \neq k$  and sufficiently large  $L$ . As a consequence, the decisions made in the Step 7 of the CFCPSC algorithm are independent of each other, and the decision threshold set to yield a target  $P_{\text{fa}}$  becomes  $\gamma = I_{(1-P_{\text{fa}})^{1/L}}^{-1}(\alpha, \beta)$ , where  $I_x^{-1}(\alpha, \beta)$  is the inverse regularized incomplete Beta function.

In the proposed WCFCPSC algorithm, the conditional CDF of  $r_\ell^{\text{avg-w}} = w_\ell r_\ell^{\text{avg}}$ , that is,  $F_{r_\ell^{\text{avg-w}}}(y) = \Pr[r_\ell^{\text{avg-w}} < y]$ , can be found applying a simple transformation of variables, yielding

$$F_{r_\ell^{\text{avg-w}}}(y) = I_{y/w_\ell}(\alpha, \beta), \quad (4)$$

for  $0 < y < w_\ell$ . Analogously, the conditional PDF of  $r_\ell^{\text{avg-w}}$  is

$$f_{r_\ell^{\text{avg-w}}}(y) = \frac{(y/w_\ell)^{\alpha-1} (1 - y/w_\ell)^{\beta-1}}{B(\alpha, \beta)w_\ell}. \quad (5)$$

Let the random vector  $\mathbf{r}^{\text{avg-w}} = [r_1^{\text{avg-w}}, \dots, r_L^{\text{avg-w}}]^T$ . Under the same independence assumption for sufficiently large  $L$ , the joint PDF is given by  $f_{\mathbf{r}^{\text{avg-w}}}(y_1, \dots, y_L) = \prod_{\ell=1}^L f_{r_\ell^{\text{avg-w}}}(y_\ell)$ , and the joint CDF is  $F_{\mathbf{r}^{\text{avg-w}}}(y_1, \dots, y_L) = \prod_{\ell=1}^L F_{r_\ell^{\text{avg-w}}}(y_\ell)$ . Hence, the probability of false alarm of the WCFCPSC algorithm for a given decision threshold  $\gamma$  becomes  $P_{\text{fa}} \approx 1 - \prod_{\ell=1}^L F_{r_\ell^{\text{avg-w}}}(\gamma)$ , yielding

$$P_{\text{fa}} \approx 1 - \prod_{\ell=1}^L I_{\gamma/w_\ell}(2VU, NU - 2VU). \quad (6)$$

Figs. 2 and 3 show theoretical and simulated  $P_{\text{fa}}$  versus  $\gamma$  for the WCFCPSC with weights given by (3) (hereafter referred to as the suboptimal WCFCPSC), and the CFCPSC, for  $L = 10, 20, 40, 80$ , and for  $U = 5$  (Fig. 2) and  $U = 10$  (Fig. 3). The theoretical results were obtained from (6) for the WCFCPSC, and from the same equation with  $\gamma/w_\ell$  replaced by  $\gamma$  in the case of the CFCPSC, using the built-in MATLAB function `betainc`. Notice that theoretical and simulated curves are very close to each other, better matching for larger values of  $L$ , since  $\rho_{i,k} \rightarrow 0$  as  $L$  increases, for  $i \neq k$ . Notice also that

the gaps between theoretical and simulated results are smaller in the case of the WCFCPSC. The effect of a larger  $U$  is to reduce  $P_{\text{fa}}$  for a given  $\gamma$ , as expected.

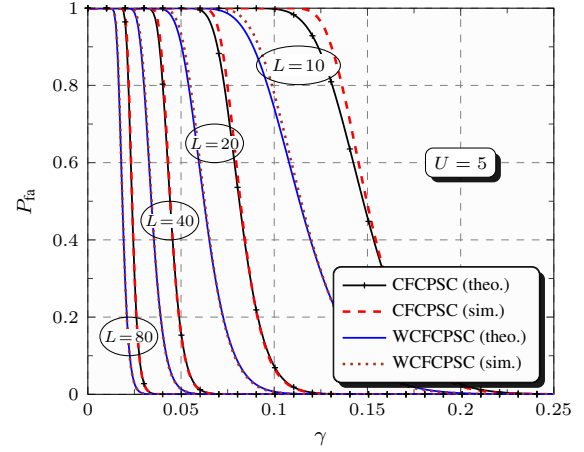


Fig. 2: Simulated and theoretical  $P_{\text{fa}}$  versus  $\gamma$  for the CFCPSC and the suboptimal WCFCPSC. This figure is better viewed in color.

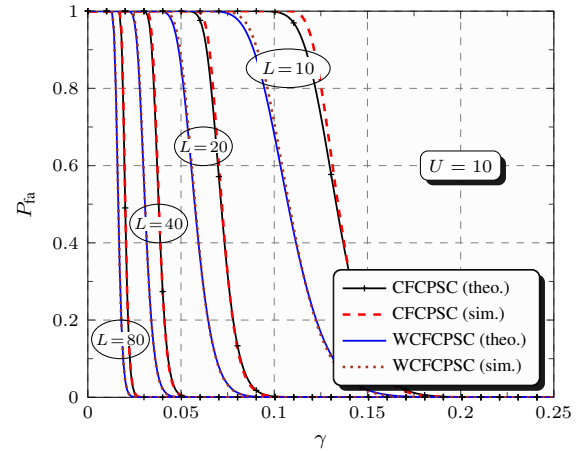


Fig. 3: Simulated and theoretical  $P_{\text{fa}}$  versus  $\gamma$  for the CFCPSC and the suboptimal WCFCPSC. This figure is better viewed in color.

## V. PERFORMANCE RESULTS

This section presents computer simulation results in terms of AUCs, comparing the performances of the CFCPSC, the near-optimal WCFCPSC (using the PSD-shaped weights) and the suboptimal WCFCPSC (using the linearly-decaying weights given in (3)). Each AUC value was generated from 100,000 simulation runs, using the MATLAB software. The PU signal was a baseband QPSK signal with  $S$  samples per symbol. Each SU, from a total of five or ten, collects  $N = 2L$  samples of the received signal during each sensing event. The collected samples are assumed to be transmitted to the FC via error-free orthogonal control channels. The scenarios analyzed are the same considered in Tables I and II. The average SNRs across the SUs were set to  $\Gamma = -6.46, -8.93, -11.74, -13.4$  dB for  $U = 5$ , and  $\Gamma = -8.37, -10.77, -13.57, -15.17$  dB for  $U = 10$ , respectively for  $N = 20, 40, 80, 160$ . As before, these SNRs guarantee approximately the same best performance for

TABLE III: Performances of the CFCPSC, the near-optimal WCFCPSC and the suboptimal WCFCPSC in terms of AUC, for  $U = 5$  and  $U = 10$  primary users. The gray-shaded values are the largest in each category.

$L \backslash S$		4	5	8	10	16
10	CFCPSC	0.739; 0.738	0.787; 0.789	–	0.846; 0.847	–
	near-optimal WCFCPSC	<b>0.862; 0.859</b>	<b>0.900; 0.898</b>	–	<b>0.947; 0.947</b>	–
	suboptimal WCFCPSC	0.842; 0.827	0.890; 0.881	–	0.942; 0.942	–
20	CFCPSC	0.683; 0.683	0.722; 0.724	–	0.836; 0.840	–
	near-optimal WCFCPSC	<b>0.824; 0.817</b>	<b>0.867; 0.864</b>	–	<b>0.947; 0.947</b>	–
	suboptimal WCFCPSC	0.818; 0.806	0.861; 0.853	–	0.943; 0.944	–
40	CFCPSC	0.600; 0.590	–	0.700; 0.695	–	0.805; 0.804
	near-optimal WCFCPSC	0.713; 0.694	–	<b>0.869; 0.861</b>	–	<b>0.949; 0.947</b>
	suboptimal WCFCPSC	<b>0.747; 0.734</b>	–	0.866; <b>0.866</b>	–	0.936; 0.939
80	CFCPSC	0.566; 0.563	–	0.654; 0.651	–	0.785; 0.786
	near-optimal WCFCPSC	0.655; 0.640	–	<b>0.827; 0.815</b>	–	<b>0.947; 0.946</b>
	suboptimal WCFCPSC	<b>0.716; 0.706</b>	–	<b>0.840; 0.842</b>	–	0.931; 0.937
$U$		5; 10	5; 10	5; 10	5; 10	5; 10

all  $N$ , which is  $\approx 0.95$  for  $L = 10, 20, S = 10$ , and  $L = 40, 80, S = 16$ , considering the near-optimal weights.

Table III presents the performance results, evidencing the superiority of the WCFCPSC scheme over the CFCPSC. Moreover, it can be seen that the suboptimal WCFCPSC performs quite close to the near-optimal one, meaning that the weights as given by (3), which are very simple to compute, are strongly recommended due to the high complexity of finding the near-optimal weights.

The performances achieved with the suboptimal weights slightly overcame those attained with the near-optimal weights in some cases corresponding to very low SNRs. This fact gives even more value to the choice of linearly-decaying weights, at the same time not contradicting the near-optimality of the PSD-shaped weights. Hence, from another point of view, the linearly-decaying weights can be also considered near-optimal.

Now, the performance improvement effect of a larger  $U$  can be observed by noticing in Table III that the close values of AUCs for  $U = 5$  and  $U = 10$  were attained with SNR values in the case of  $U = 10$  approximately 2 dB smaller than in the case of  $U = 5$ .

## VI. CONCLUSIONS

This correspondence proposed the weighted CFCPSC algorithm, aiming at superior spectrum sensing performances when compared with the original CFCPSC algorithm. Near-optimal and suboptimal versions of the weights were analyzed, unveiling that the suboptimal ones are preferred, since they are capable of achieving performances very close to those attained with the near-optimal weights, with practically no complexity increase with respect to the original CFCPSC algorithm. Expressions for the distributions of the test statistics and for the probability of false alarm were also derived and validated by simulation results.

## REFERENCES

- [1] Y. Chen and H. S. Oh, "A survey of measurement-based spectrum occupancy modeling for cognitive radios," *IEEE Commun. Surveys Tuts.*, vol. 18, no. 1, pp. 848–859, Firstquarter 2016.
- [2] I. F. Akyildiz, B. F. Lo, and R. Balakrishnan, "Cooperative spectrum sensing in cognitive radio networks: a survey," *Physical commun.*, vol. 4, no. 1, pp. 40–62, Mar. 2011.
- [3] L. G. Giordano and L. Reggiani, Eds., *Vehicular Technologies: Deployment and Applications*. IntechOpen, Ltd., 2013.
- [4] R. Gao, Z. Li, P. Qi, and H. Li, "A robust cooperative spectrum sensing method in cognitive radio networks," *IEEE Commun. Lett.*, vol. 18, no. 11, pp. 1987–1990, Nov. 2014.
- [5] R. C. D. V. Bomfin, R. A. A. de Souza, and D. A. Guimarães, "Circular folding cooperative power spectral density split cancellation algorithm for spectrum sensing," *IEEE Commun. Lett.*, vol. 21, no. 2, pp. 250–253, Feb. 2017.
- [6] R. C. D. V. Bomfin, D. A. Guimarães, and R. A. A. de Souza, "On the probability of false alarm of the power spectral density split cancellation method," *IEEE Wireless Commun. Lett.*, vol. 5, no. 2, pp. 164–167, Apr. 2016.
- [7] L. S. Costa, R. C. D. V. Bomfin, D. A. Guimarães, and R. A. A. de Souza, "Performance of blind cooperative spectrum sensing under nonuniform signal and noise powers," *J. of Commun. and Inform. Syst.*, vol. 33, no. 1, Jun. 2018.
- [8] E. M. de Almeida, L. S. Costa, R. A. A. de Souza, and D. A. Guimarães, "Performance analysis of the circular folding cooperative power spectral density split cancellation algorithm for spectrum sensing under errors at the quantized report channel," in *2018 IEEE 10th Latin-American Conf. on Commun. (LATINCOM)*, Nov. 2018, pp. 1–6.
- [9] L. S. Costa and R. A. A. de Souza, "Performance-traffic-trade-off of two novel hard decision and two soft decision fusion periodogram-based algorithms for cooperative spectrum sensing under unreliable reporting channel," *IET Microwaves, Antennas and Propagation*, vol. 14, no. 14, pp. 1683–1695, Nov. 2020.
- [10] T. Cadwallader-Olsker, "What do we mean by mathematical proof?" *J. of Humanistic Math.*, vol. 1, no. 1, pp. 33–60, Jan. 2011.
- [11] S. A. Lesik, *Applied statistical inference with MINITAB*. CRC Press, 2009.
- [12] I. Gradshteyn and I. Ryzhik, *Table of Integrals, Series, and Products*, 7th ed. Wiley, 2007.